W.C. PEI, Y. HU, G.F. CUI, H. C.JI

ISSN 0543-5846
METABK 63(1) 149-152 (2024)
UDC – UDK 669.715.721.782:621.791.052/546.293:629.118.3:518.1=111

# NUMERICAL SIMULATION OF WELDING OF INTERSECTING LINE JOINTS OF 6061-T6 ALUMINUM ALLOY BICYCLE FRAME

Received – Primljeno: 2023-06-20
Accepted – Prihvaćeno: 2023-08-25
Preliminary Note – Prethodno priopćenje

The joints of aluminum alloy frames are usually welded by manual TIG welding. In order to study the distribution law of welding stress level and welding temperature field of intersecting joints of 6061-T6 aluminum alloy bicycle frames, a intersecting joints model of welding parts was established by Finite Element Model (FEM), Software. Based on ABAQUS software, the welding temperature field and welding stress field were studied and analyzed by using direct thermal coupling method. The accuracy of welding simulation is fully verified, which can meet the simulation requirements required for the subsequent optimization process design, and achieve the purpose of shortening the time required for the accumulation of practical inspection.

*Keyword*: aluminum alloy 6061-T6, bicycle frame, argon arc welding, numerical simulation, Finite Element, model (FEM)

## INTRODUCTION

The 6061-T6 series Al-Mg-Si alloy has good comprehensive properties and good properties in strength and plasticity[1]. In the aluminum alloy bicycle frame, manual argon arc welding ( TIG ) is usually used for welding, and the main part of the welding is the intersecting line node path of the frame (Figure 1). Therefore, this paper studies and analyzes the distribution of welding stress field and welding temperature field of intersection line node of 6061-T6 aluminum alloy frame, which provides a basis for the improvement of welding method and process of intersection line node in aluminum alloy workshop [2]. The chemical composition of aluminum alloy 6061-T6 is shown in Table 1.

Table 1 **Chemical composition of 6061-T6 aluminum alloy /wt. %**

| Si | Fe | Cu | Mn | Mg |
|---|---|---|---|---|
| 0, 4~0, 8 | 0, 7 | 0, 15~0, 4 | 0, 15 | 0, 8~1, 2 |
| Cr | Zn | Ti | Al | Other |
| 0, 04~0, 3 | 0, 25 | 0, 15 | residual | 0, 15 |

## THE ESTABLISHMENT OF FINITE ELEMENT MODEL

The material selected in this paper is 6061-T6 aluminum alloy. According to the solid frame, the component modeling is carried out. In order to facilitate the specific analysis, a simple local modeling of the main welding parts is carried out. Taking the welding part of the frame intersecting line as the main research object, the welding analysis of the node position of the frame intersecting line is carried out. As shown in Figure 2, the weld area in the Figure is highlighted.

**Figure 1** 6061-T6 aluminum alloy bicycle frame

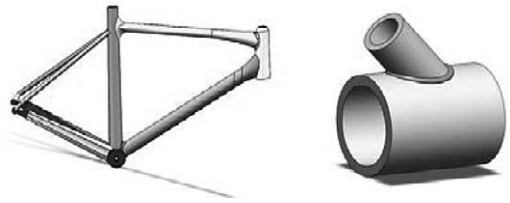

**Figure 2** Frame intersecting line node welding part and welding model

In the numerical simulation of welding, the direct thermal-mechanical coupling method can be more convenient for numerical simulation. By using a unit type, two physical field problems can be solved, and the real coupling between heat and structure can be realized. By consulting the relevant literature and using JMatPro software to extrapolate the required material parameters, the welding numerical simulation is completed[3]. In Figure 3, argon arc welding parameters are used for numerical simulation. Table 2 is argon arc welding parameters.

According to the observation of arc shape and energy distribution characteristics in the process of aluminum al-

W.C. Pei, Y. Hu, H.C Ji, (E-mail: jihongchao@ncst.edu.cn), North China University of Science and Technology, Hebei, Tangshan, China. G.F. Cui, Tangshan Longquan Machinery Co., Ltd., Tangshan, Hebei, China.

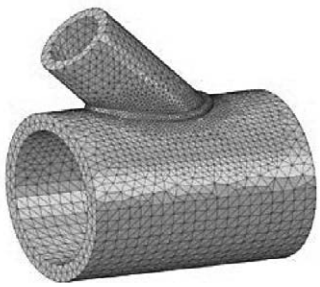

**Figure 3** Mesh division of welding model

Table 2 **Welding parameters**

| Welding manner | Welding current / A | Arc voltage / V | welding speed / mm·s$^{-1}$ |
|---|---|---|---|
| TIG | 80 | 12 | 5 mm/s |

loy welding test, the heated part will form the phenomenon of heat tailing. Therefore, the we welding heat source of this numerical simulation adopts the double ellipsoid heat source model, as shown in Figure 4[4].

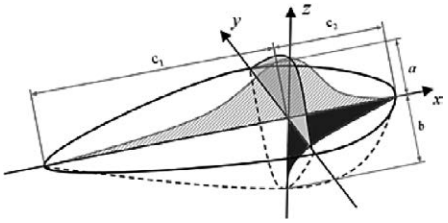


**Figure 4** Double ellipsoid heat source model and its parameters

The heat flux distribution function of the double ellipsoid heat source model is expressed as:

$$q(x,y,z,t)=\frac{6\sqrt{3}f_f}{abc_1\pi\sqrt{\pi}}\exp(-3(\frac{x^2}{a^2}+\frac{y^2}{b^2}+\frac{(z-vt)^2}{c_1^2}))$$

$$q(x,y,z,t)=\frac{6\sqrt{3}f_r}{abc_2\pi\sqrt{\pi}}\exp(-3(\frac{x^2}{a^2}+\frac{y^2}{b^2}+\frac{(z-vt)^2}{c_2^2}))$$

In the formula: $f_f$, $f_r$ is the heat flux distribution coefficient, $f_f + f_r = 2$, where $f_f$ takes 0,6, $f_r$ takes 1,4 ; a, b, $c_1$ and $c_2$are the geometric dimensions of the molten pool. According to the above analysis, the heat source program is written and debugged by Fortran language.

## NUMERICAL SIMULATION RESULTS AND ANALYSIS

The heat source movement trajectory of the weld during welding and the distribution of the temperature field at different times are shown in Figure 5. The dynamic process of temperature field change in the welding process can be clearly observed. Since the heating rate of the weldment is much larger than the cooling rate, the isotherms in the forward direction of the heat source are dense, and the rear isotherms are sparse[5] [6]. The heat source morphology is shown in Figure 6.

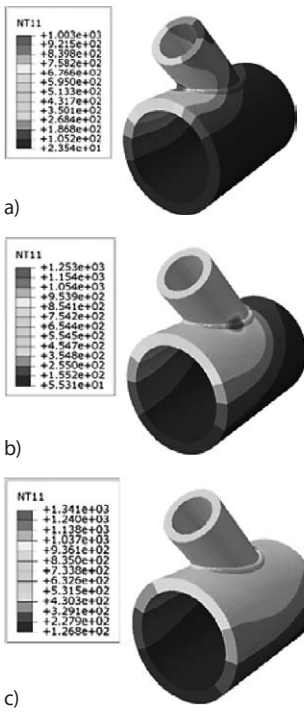


(a) Welding time is 3 s (b) Welding time is 6 s
(c) Welding time is 9 s

**Figure 5** Results of weld temperature field model

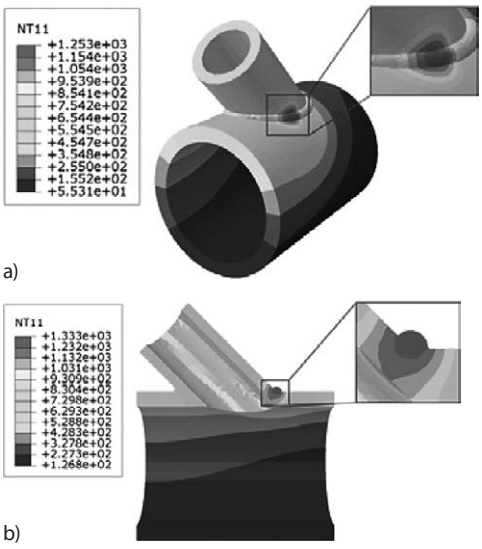


(a) Surface topography of heat source
(b) Heat source molten pool morphology

**Figure 6** Welding heat source cloud diagram and heat source molten pool morphology

It can be intuitively observed from Figure 7 that the temperature change process of each point on the weld is extremely rapid, and the heating rate is greater than the cooling rate. At the same time, the development trend of the temperature cycle curve of each point is consistent. When the heat source acts, the action point rises rapidly, and then immediately enters the cooling stage. After the welding is completed, the continuous cooling is slowly carried out.

From the stress cloud diagram of the above three time nodes in Figure 8, it can be intuitively observed that in the equivalent stress cloud diagram, each weld

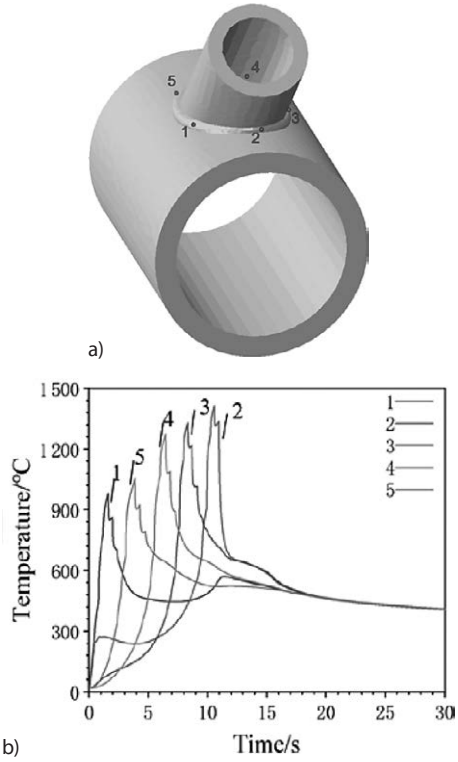


(a) Selection of weld nodes (b) Temperature cycling curve

**Figure 7** Selection of nodes and temperature cycling profiles at the weld seam

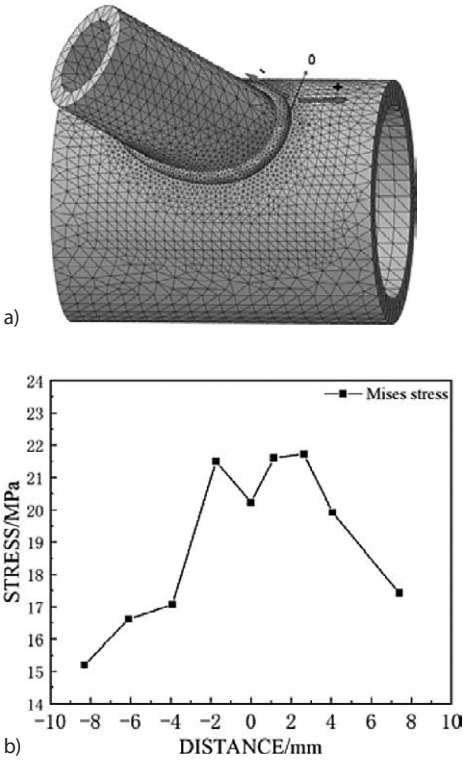


(a) Selection of weld nodes (b) Stress values at weld nodes

**Figure 9** Selection of stress field nodes and stress value of weld after welding

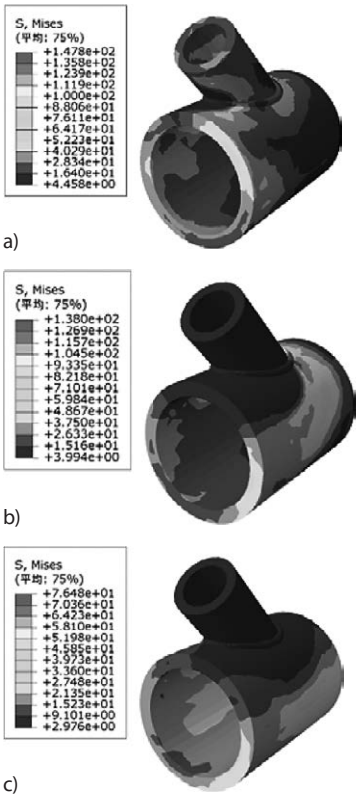


(a) Welding time is 3 s (b) Welding time is 6 s (c) Welding time is 9 s

**Figure 8** Stress field model results of oblique column weld

seam is distributed with concentrated and high welding residual stress. Due to the highest temperature at the center of the welding heat source during welding, the base metal at the center of the heat source during welding is in a molten state, so the stress level is extremely low or negligible. It can be seen from Figure 9 that the residual stress is mainly concentrated in the weld part, showing the distribution trend of residual stress from the middle part of the weld to the two ends of the weld from high to low.

## CONCLUSION

By studying the TIG welding process of 6061-T6 aluminum alloy frame, the numerical simulation of welding is completed by Fortran heat source subroutine in ABAQUS environment. The distribution of welding temperature field and welding stress field at the joints of the intersecting line of the frame is studied and analyzed. During the welding process, with the action of the heat source, the action point rises rapidly, and then immediately enters the cooling stage. After the welding is completed, the continuous cooling is slowly carried out. The welding stress is mainly concentrated in the weld part, showing the distribution trend of residual stress from the middle part of the weld to the two ends of the weld from high to low. Through the observation and analysis of the heat source morphology, temperature field and stress field in the numerical simulation of welding, it is shown that the model can well reflect the welding process of TIG welding 6061-T6 aluminum alloy bicycle frame. It can meet the simulation requirements required for subsequent optimization of process

design, and achieve the purpose of shortening the time required for practical test accumulation.

## Acknowledgments

This work is supported by the National Natural Science Foundation of China (No. 51704052) and the Natural Science Foundation of Hebei Province (E2020318006), and the Innovation and Entrepreneurship Training Program for University Students (R2020024) was successfully carried out based on the support of this work.

## REFERENCES

[1] F. Ma, Study on numerical simulation ofwelding Deformation and residual stress ofaluminum alloy based on ABAQUS [D]. Chongqing Jiaotong University, 2016.

[2] Li Y, Zou W, Lee B, et al. Research progress of aluminum alloy welding technology [J]. The International Journal of Advanced Manufacturing Technology 109 (2020) 5, 1207-1218.

[3] Bansal A, Kumar M. S, Shekhar I, et al. Effect of welding parameter on mechanical properties of TIG welded AA6061[J]. Materials Today: Proceedings 37 (2021), 2126-2131.

[4] Ravisankar A, Velaga S.K, Rajput G, et al. Influence of welding speed and power on residual stress during gas tungsten arc welding (GTAW) of thin sections with constant heat input: A study using numerical simulation and experimental validation[J]. Journal of Manufacturing Processes 16 (2014) 2, 200-211.

[5] Arora H, Basha K. M, Abhishek D. N, et al. Welding simulation of circumferential weld joint using TIG welding process[J]. Materials Today: Proceedings (2022) 50, 923-929.

[6] Tsirkas S. A, Numerical simulation of the laser welding process for the prediction of temperature distribution on welded aluminium aircraft components[J] Optics & Laser Technology (2018) 45-56.

**Note:** The responsible translator for English language is M.M. LI -North China University of Science and Technology, China